Id.: CR30

3D IMAGE MODELING FOR THE PRODUCTION OF THE ICRP MALE REFERENCE PHANTOM BY ADDITIVE MANUFACTURING

Hirys Sales[1], Ester M. R. de Andrade[1] ; Bruno M. Mendes[1]
[1]Centro de Desenvolvimento da Tecnologia Nuclear – CDTN/CNEN – Universidade Federal de Minas Gerais – UFMG - Avenida Presidente Antônio Carlos, 6627, Pampulha, Belo Horizonte, MG.

hirys.sales@cdtn.br

Keywords: Internal Dosimetry; Phantom; 3D Print; Additive Manufacturing

ABSTRACT

The Whole-Body Counter (WBC) is an in vivo monitoring system designed for the detection of internal contamination with radioactive material. The in vivo monitoring methodology is particularly applicable to occupationally exposed individuals, but it can also be utilized for the general public in the event of accidents. The calibration of this type of counting system uses anthropomorphic physical phantoms and/or mathematical methods, such as the Monte Carlo simulations with computational phantoms. Normally, the physical phantoms have a known amount of activity of a specific radionuclide homogeneously distributed to allow vivo counters calibration. The ICRP provides the voxelized male and female adult reference phantoms in text format files. These are computer-based simulators with human geometry and constituted by tissues with heterogeneous compositions and densities to enhance their realism. Additive manufacturing enables the physical reproduction of ICRP computational models with exceptional geometric fidelity. The objective of this study was to develop imaging manipulation techniques to generate stereolithography (STL) parts for the 3D printing a male physical phantom based on the Reference Computational Phantom (RCP_AM) model provide in the ICRP 110 publication. The text format provided by the ICRP was transformed into a three-dimensional image using a C^{++} code. Subsequently, the image was subjected to a Laplacian smooth filter in MeshLab software. The resulting image was then divided into right and left parts using the FreeCAD software, where it was subsequentially sectioned into 22 distinct parts. Each portion was fitted with a puzzle-like configuration, allowing them to be easily joined together in the moment of the calibration. The Meshmixer software was used to manipulate each of the 22 parts individually, resulting in the creation of hollow parts with a 7 mm wall and a cover lid. A step-shaped fitting was created to improve the sealing between the lids and the hollow parts. All lids were equipped with a small hole, allowing for the safe filling of radioactive material. A specialized cap was designed to seal these holes. All the parts were successfully produced with the novel methodology for manipulating STL images. This new methodology offers greater ease of assembling the model and better fit among the parts. In this way, it represents an evolution in comparison to our previous work on producing physical models through 3D printing.

1. INTRODUCTION

The Whole-Body Counter (WBC) is an in vivo monitoring system that enables the quantification and identification of radioisotopes incorporated in to an individual. The system is a widely used tool in internal dosimetry. In vivo monitoring is typically employed for both occupationally exposed individuals and the general public [1, 2].

The calibration of the WBC is necessary to make possible to convert the counting rate obtained by the system when monitoring an individual into the activity present in that same individual at the time of incorporation. It is possible to obtain calibration coefficients, CC, for WBC by relating the count rate obtained for a given physical model positioned inside the counter with the activity of a given radioisotope distributed in such a model. The CC of in vivo monitoring systems depend on several parameters such as: i) counting geometry; ii) sensitivity, response time and energy resolution of the detector; iii) type of particle emitted and its energy; and iv) probability of emission per decay. The bed geometry exhibits good detection efficiency and provides a consistent response for radionuclides distributed uniformly on the body [1, 3]

The most prevalent detectors used in WBC are NaI(TI) scintillators and HPGe semiconductors [1]. It is important to note that the size of the detectors has an impact on the counting efficiency of the system [1, 2, 3]. The WBC used in this study is equipped with an 8" x 4" (20.32 x 10.16 cm) NaI(TI) detector and has a bed-type configuration. The detector is positioned 53.2 cm above the bed [4].

The Whole-Body Counter can be calibrated using a variety of methods, including point sources, volunteers and patients, anthropomorphic physical simulators, and mathematical simulation (Monte Carlo Method - MC) [1, 3, 5]. Physical phantoms have the peculiarity of subjectivity in representing the human body, as they are mostly composed of geometric shapes, such as the BOMAB and IGOR phantoms[1, 3, 5, 6, 7]. In addition to geometric issues, physical phantoms assume that the distribution of incorporated nuclides is homogeneous, which in several cases do not match with the real biodistribution patterns. These aspects increase the measurements uncertainties. However, MC codes could be used to generate more personalized data, once the simulations are well validated with the physical models[2, 3, 5].

Additive manufacturing has played a significant role in the production of new simulators for various applications, including dosimetry in radiotherapy and image quality control for radiological equipment. This technique allows for the exclusive modelling of phantoms, facilitating the creation of human anatomically similar simulators. Several studies have used 3D printing and investigated its efficiency in geometrically replicating human characteristics [5, 8, 9, 10].

The objective of this study was to develop imaging manipulation techniques to generate stereolithography (STL) parts for the production of a male physical phantom based on the Reference Computational Phantoms (RCP_AM) model from the ICRP, using 3D printing. The male phantom will be used in the calibration of Whole-Body Counters. It aims to mitigate uncertainties associated with body geometry, resulting in more accurate dosimetry. Furthermore, the objective is to enhance accessibility to calibration physical phantoms and to facilitate standardization in the calibration of WBC systems.

2. METHODOLOGY

The Reference Male Phantom for Internal Dosimetry (RMPID) was developed based on the ICRP-110 Adult Male Reference Computational Phantom (RCP_AM) [11]. The word “reference” was used because the model will be based in the ICRP reference phantom. The male computational phantom was produced from a set of whole-body clinical computed tomography images of a 38-year-old individual with a height of 176 cm and a mass of just under 70 kg. The resulting phantom has the same height, differing only in weight (73 kg).

The reference male was positioned in a supine position with his arms parallel to his body during the computed tomography (CT) scan. The data set consisted of 220 slices of 256 x 256 pixels. The original voxel size was 8 mm high, with an in-plane resolution of 2.08 mm, resulting in a voxel volume of 34.6 mm³ [11]. Tab. 1 describes the main physical characteristics of the RCP_AM.

Tab. 1. Main characteristics of the RCP_AM/ICRP.

Characteristic	Male Phantom
Height (m)	1.76
Mass (kg)	73.0

Number of tissue voxels	1,946,375
Slice thickness (voxel height, mm)	8.0
Voxel in-plane resolution (mm)	2.137
Voxel volume (mm3)	36.54
Number of columns	254
Number of rows	127
Number of slices	220 (+2)*

*Additional slices of skin at the top and bottom (Adapted from ICRP 2009)

As can be observed in Fig.1, this computational phantom was segmented with different organs and tissues, with respectives densities and elemental compositions. However, in this study, the interest resides mainly in external shape of the model. Thus, the RMPID phantom was made to be homogeneous inside. The RMPID simulator was designed to be an active calibration phantom, which means that it will contains a known amount of activity of a specific radionuclide. These characteristics will allow its use for the calibration of in vivo systems [5, 6].

Fig. 1. Front view of the ICRP-AM, a voxel model that represents the adult ICRP reference ICRP male [12].

2.1 Production Stages Of The Reference Male Phantom For Internal Dosimetry-RMPID.

The initial step was to transform the text file (RCP_AM) provided by the ICRP into a three-dimensional image [10]. The C^{++} program reads the text file of the reference male phantom and then generates a three-dimensional matrix, each voxel "filled" with the corresponding tissue codes. To accomplish this task, the code employs the CImg library, which is utilized for create and manipulate of RAW-type images [13].

In the ImageJ software [14], the sequence of RAW axial images was extracted and binarized, thus the heterogeneous tissue structures of the computational phantom were changed into a uniform solid piece, while preserving the original external shape and geometry of the phantom. To remove the pixelated appearance of the simulator, the Laplacian Smooth filter was applied in the MeshLab software [15], thereby smoothing the surface and thereby improving the appearance of the simulator in 3D printing.

The binarized and smoothed image of the phantom was imported into the FreeCAD software [16]. The simulator was divided into two portions, corresponding to the right and left sides. Each side was divided in parts with 20 cm height, in alignment with the dimensions of the 3D printer's footprint, as described in Fig. 2.

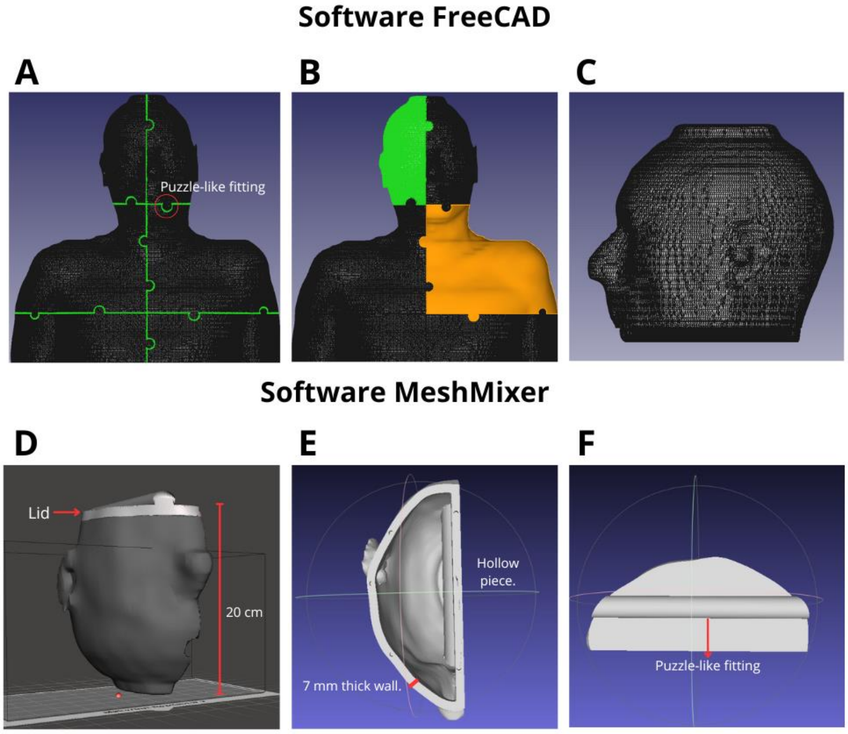

Fig. 2. A-B) Division of the 3D image using FreeCAD software. Main division Right and Left, note the separation between the 22 portions with fittings between them. C) Product of the division of the portions, the image shows the Right part of the head. D) Division of the part into a lid and a hollow part. E) Hollow piece. F) Lid, note the presence of the puzzle-like fitting.

Subsequently, fittings were designed in a manner analogous to puzzle pieces. For smaller regions, the radius of the fittings was set to 8 mm, while for larger regions, it was set to 10 mm. These fittings were positioned between the divisions of the pieces at a distance proportional to the size of the region. The fittings were then extracted from the phantom geometry, resulting in the formation of 22 discrete components with interconnecting joints.

To the phantom to be suitable for use in internal dosimetry, it must have a hollow interior. The purpose of the empty chamber is to be filled with equivalent tissue material mixed with a radionuclide. Once the fittings have been created, it is necessary to export the parts separately to facilitate individual manipulation in the Meshmixer software [17]. As illustrated in Fig. 2, at this step, the Hollow function was applied, thereby transforming the solid piece into a hollow portion with a 7 mm wall thickness. Subsequently, the hollow portion was divided into two distinct components: a lid and a hollow part. It is important to note that all 22 parts will be subjected to the same process, resulting in the creation of a lid and a hollow portion.

To prevent potential accidents, it is important to implement mechanisms that mitigate the risk of spillage and leaking while filling the parts with radioactive material. To this end, the main lid of the hollow portions was given a 10 mm hole and a cap to seal the part without excess air after filling. The hole was created using FreeCAD software, where two cylinders were generated, with a radius of 10 mm and 8 mm (Fig.3), joined together to form a single geometry, which was then positioned and subtracted from the main lid. As the 3D printer has a certain imprecision about the size of the print, it was necessary to reduce the radius of the cylinders so that the cap could fit loosely into the hole (radius of 9.5 mm and 7.5 mm).

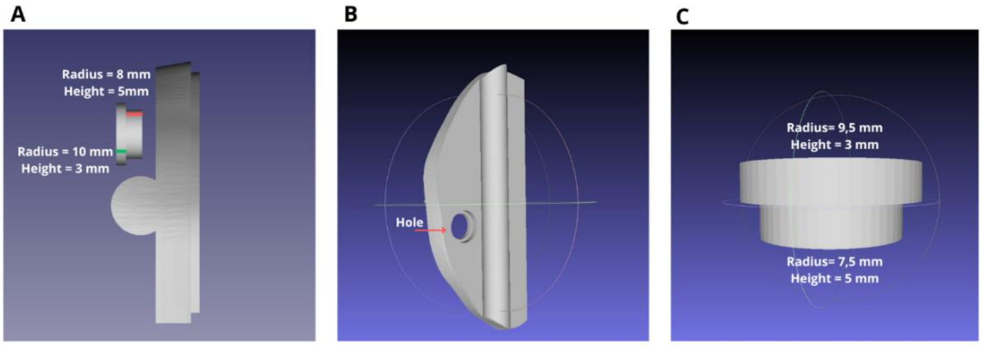

Fig. 3. Illustration of the methodology for the creation of the aperture in the lid. A) The dimensions and position of the mold for the hole. B) Lid with hole. C) Lid reduced to fit the hole.

In the production of the fitting between the lid and the hollow part, two potential methods were tested. In the first one, with the FreeCAD software, pins were designed and subsequently attached to the edge of the lid. The geometry of the pins was then subtracted from the 7 mm wall of the hollow part to create the fitting. The Fig. 4 shows the result of this process. The scale of the pins attached to the lid was adjusted to ensure proper fitting. The part was then printed at full scale for fitting validation. However, it was found that this approach did not achieve the goal of effectively sealing the part to prevent radioactive material leakage. Consequently, it was decided to adopt a new method for reconfiguring the fittings.

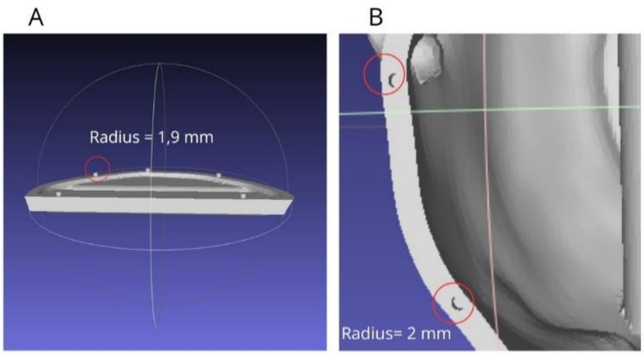

Fig. 4. First method of pins fitting in the lid and in the hollow part. A) Pins positioned in the lid B) Subtraction of the pins in the 7 mm wall of the hollow part.

To further improve safety, the geometry of the lid was redesigned, generating a raised area 5 mm apart from the main edge of the lid. As shown in Fig.5A, in the Meshmixer software, the edge of the lid was cut off, producing a Slice that was separated from the rest of the geometry. In the FreeCAD software, the Slice was rescaled making the XYZ = 1 mm axes, to reduce the geometry the scale was changed to X = 0.95 mm Y = 0.97 mm and Z = 5 mm resulting in a piece smaller than the main edge of the lid. The next step was to centrally position the Slice (Fig.5B) on the lid and apply the union of the two geometries. The result is shown in Fig.5C. Still in the FreeCAD software, the new geometry of the lid must be subtracted from the structure of the hollow part, this will form a 7 mm wall recess, as shown in Fig.5D and 5E.

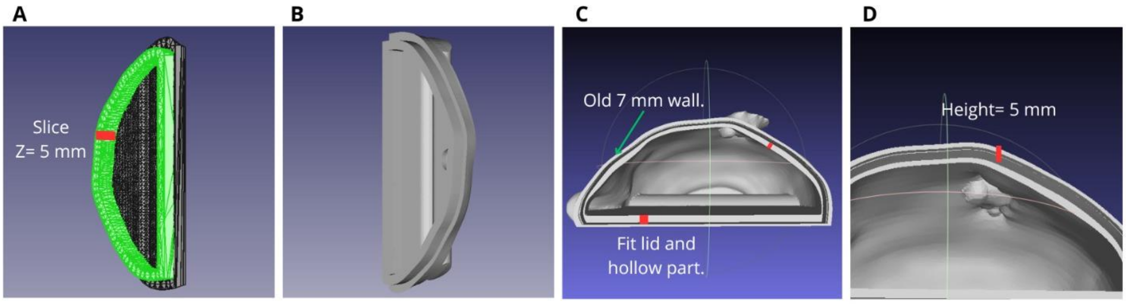

Fig. 5. Process of creating the step-shaped fitting in the lid and in the hollow part. A) Slice taken from the geometry of the lid and positioned with new scale. B) Final product of the action, lid with 5 mm protrusion. C-D) Result of subtracting the 5 mm fitting from the 7 mm wall of the hollow piece.

The 5 mm border created on the lid was reduced to the following dimensions: X = 0.92 mm, Y = 0.94 mm and Z = 5 mm. This reduction process was necessary so that the structure can fit properly into the space created in the head by subtracting the previous scale.

The pieces were printed to validate the functionality of the fittings, including a miniature reduced to 25% of the original scale, which was used to validate the puzzle-type fitting. In full scale, caps and sealing plugs were printed, as well as a hollow piece. The material used for printing was PLA (polylactic acid) produced by 3D Lab (3D Printing Solutions) and the parameters used for printing are those used in RFPID production [5].

3. RESULTS

The proposal to create a fitting between the 20 cm portions was informed by the experience gained in the creation of the RFPID, where the phantom parts were fixed with heat-shrink plastic [5]. This prompted a discussion regarding the potential modifications to be made to facilitate the manipulation of the simulator and the anticipated behavior when assembling the pieces in the supine position on the WBC. Furthermore, the security of the lid and hollow part fittings was enhanced, ensuring that the newly designed shape facilitates more efficient sealing of the phantom.

As a final result of the manipulation, a lid was obtained that allows for the internal sealing of the phantom. The scale of the fitting was altered (as observed in Fig. 6) to ensure proper positioning within the hollow portion, facilitating the gluing of the lid.

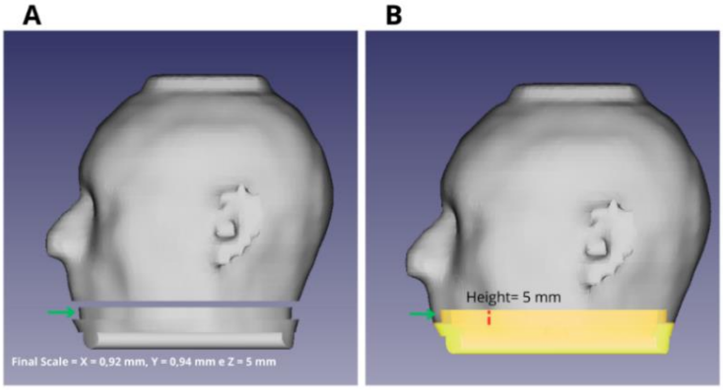

Fig. 6. Geometry of the end cap. A) Note that the 5 mm high recess will be inside the hollow part. B) Demonstration of the internal position of the recess after closing the part.

The printed parts for validating the fittings are represented in Fig.7. The puzzle-type fitting was validated with the miniature print (Fig. 7A and 7B), which facilitated the handling of the parts and promoted better fit between them. The full-scale portions allowed for the validation of the geometry and verification of the necessary modifications (Fig. 7C and 7D). Among the two fitting tested between the lid and the hollow portion, the sealing objective was achieved through the second methodology described in Fig.5. Fig. 7E, 7F, and 7G illustrate the final product of the phantom's geometry. Nevertheless, additional tests are still underway to verify the applicability of the fittings after the application of resin, which will serve as a waterproofing agent.

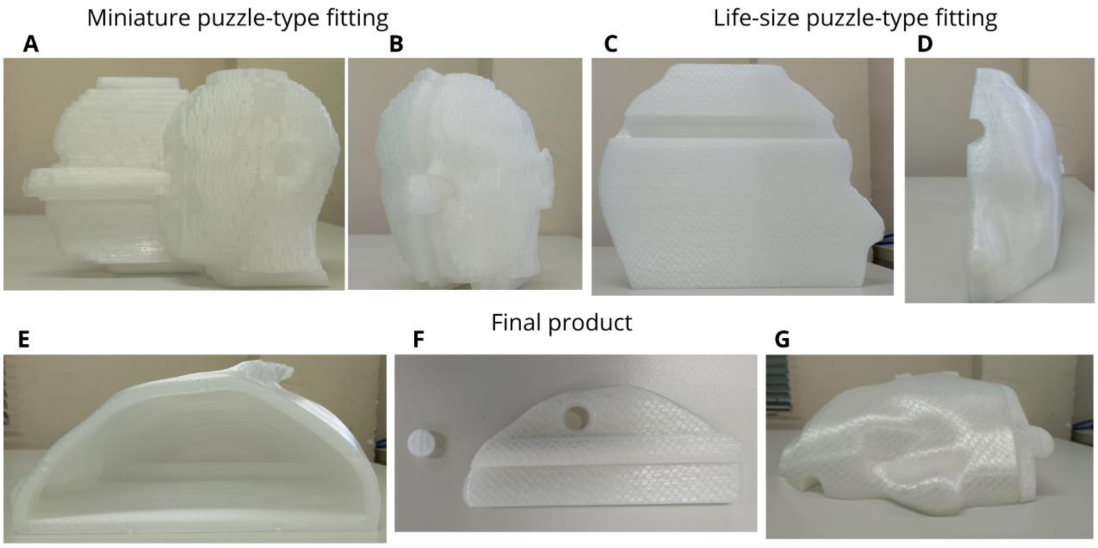

Fig.7. Printing of parts for the validation of the proposed fitting system. A-B) Miniature of the phantom's head produced to validate the puzzle-type fitting. C-D) Full-size part printed for geometry verification and fitting test between the lid and the hollow piece. E-F-G) Demonstrates the final product obtained with 3D printing, where: E) hollow piece, F) lid and sealing cap, and G) hollow piece with the lid positioned.

The software used to generate the physical male phantom is publicly accessible via the Internet, thereby ensuring the reproducibility of this process in an expedient manner. Moreover, despite the RMPID project's incomplete status, an examination of the financial aspects of RFPID production indicates that additive manufacturing enables the creation of phantoms at a reduced cost and with superior geometric precision compared to existing simulator models [5].

4. CONCLUSION

This project made a significant contribution to the development of a novel methodology for the manipulation of STL images. Consequently, the design of the phantom was reconsidered with the objective of enhancing its safety during manipulation of the simulator. The 3D images generated will enable the use of the Addictive Manufacture to fabricate the physical male phantom for in vivo system calibration. This model will have a anthropomorphic geometry and will be useful lowering uncertainties associated with phantom geometry. The proposed modeling methodology enhance safety and make the model assembly easier.

The next step is to complete the 3D printing of the RMPID phantom. Subsequently, the phantom will be filled with tissue-equivalent radioactive material, and validation tests will be conducted on the in vivo system.

ACKNOWLEDGMENTS

The following Brazilian institutions support this research project, Research Support Foundation of the State of Minas Gerais (FAPEMIG - Project APQ-03582-18), Brazilian Council for Scientific and Technological Development (CNPq) and Coordination for the Capacitation of Graduated Personnel (CAPES). This work is also part of the Brazilian Institute of Science and Technology for Nuclear Instrumentation and Applications to Industry and Health (INCT/INAIS), CNPq project 406303/2022-3.

BIBLIOGRAPHICAL REFERENCES

[1] B. M. Dantas, "Bases para a Calibração de Contadores de Corpo Inteiro Utilizando Simuladores Físicos Antropomórficos". Universidade do Estado do Rio de Janeiro, 1998.
[2] C. V.G. Ferreira *et al.*, “Monte Carlo calculation of whole body counter efficiency factors for different computational phantoms”, *Applied Radiation and Isotopes*, vol. 194, p. 110685–110685, abr. 2023, doi: 10.1016/j.apradiso.2023.110685.
[3] T. C. F. Fonseca *et al.*, “Development of a 3D human body library based on polygonal mesh surface for whole body counter set-up calibration”, *Progress in nuclear science and technology*, vol. 4, p. 614–618, abr. 2014, doi: 10.15669/pnst.4.614.
[4] F. G. Paiva *et al.*, “Calibration of the LDI/CDTN Whole Body Counter us-ing two physical phantoms”, *Brazilian Journal of Radiation Sciences*, vol. 5, nº 3, out. 2017, doi: 10.15392/bjrs.v5i3.252.
[5] E. M. R. Andrade *et al.*, “RFPID: development and 3D-printing of a female physical phantom for whole-body counter”, *Biomedical engineering and physics express*, 2024, doi: 10.1088/2057-1976/ad4650.
[6] ICRU 1992 Phantoms and computational models in therapy, diagnosis, and protection. Report 48 Report 48 International Commission on Radiation Units and Measurements.
[7] A. Kovtun, “Metrological Parameters of the Unified Calibration Whole-Body Phantom with Gamma-Emitting Radionuclides”, *Radiation Protection Dosimetry*, vol. 89, p. 239–242, jul. 2000, doi: 10.1093/oxfordjournals.rpd.a033071.
[8] D. Hong *et al.*, “Development of a CT imaging phantom of anthromorphic lung using fused deposition modeling 3D printing.”, *Medicine*, vol. 99, nº 1, jan. 2020, doi: 10.1097/md.0000000000018617.
[9] P. Kunert *et al.*, “Reproduction of a conventional anthropomorphic female chest phantom by 3D-printing: Comparison of image contrasts and absorbed doses in CT”, *Medical Physics (Lancaster)*, vol. 50, nº 8, p. 4734–4743, jul. 2023, doi: 10.1002/mp.16587.
[10] J. Colnot *et al.*, “Study of the use of gel dosimetry in combination with 3D printing phantom for personalized pretreatment QA in radiotherapy”, *Journal of Physics: Conference Series*, vol. 2167, nº 1, p. 012017–012017, jan. 2022, doi: 10.1088/1742-6596/2167/1/012017.
[11] ICRP 2009 Adult reference computational phantoms ICRP Publication 110. Ann. ICRP 39 (2)
[12] X. G. Xu e K. F. Eckerman, Orgs., *Handbook of Anatomical Models for Radiation Dosimetry*. Boca Raton: CRC Press, 2009. doi: 10.1201/EBK1420059793.
[13] https://cimg.eu/. Acesso em: 19 jul. 2024.
[14] https://imagej.net/ij/download.html. Acesso em: 19 jul. 2024.
[15] https://www.meshlab.net/ . Acesso em: 19 jul. 2024.
[16] https://www.freecad.org/. Acesso em: 19 jul. 2024.
[17] https://meshmixer.com/. Acesso em: 19 jul. 2024.